

A local eigenvector centrality

Ruaridh A. Clark^{1,*}, Francesca Arrigo², Agathe Bouis¹, Malcolm Macdonald¹

¹Centre for Signal and Image Processing, University of Strathclyde, UK

²Department of Mathematics and Statistics, University of Strathclyde, UK

*Corresponding author: Ruaridh A. Clark
University of Strathclyde, Glasgow, G1 1XJ, UK
`ruaridh.clark@strath.ac.uk`

Abstract

Eigenvector centrality is an established measure of global connectivity, from which the importance and influence of nodes can be inferred. We introduce a local eigenvector centrality that incorporates both local and global connectivity. This new measure references prominent eigengaps and combines their associated eigenspectrum, via the Euclidean norm, to detect centrality that reflects the influence of prominent community structures. In contact networks, with clearly defined community structures, local eigenvector centrality is shown to identify similar but distinct distributions to eigenvector centrality applied on each community in isolation. Discrepancies between the two eigenvector measures highlight nodes and communities that do not conform to their defined local structures, e.g. nodes with more connections outside of their defined community than within it. While reference to PageRank’s centrality assessment enables a mitigation strategy for localisation effects inherent in eigenvector-based measures. In networks without clearly defined communities, such as city road networks, local eigenvector centrality is shown to identify both locally prominent and globally connected hubs.

1 Introduction

Eigenvector centrality is a long-established network measure that assesses node centrality in terms of global reach [2, 3]. It is defined by the first, principal, eigenvector of a network’s adjacency matrix, A , that is associated with the largest eigenvalue and representative of the dominant direction of change when a vector is transformed by A . This measurement of a node’s ability to send and receive information across the whole network is primarily of interest when influence is dominated by a single central hub or when high global connectivity reduces the relevance of local structures. However, it is often the case for real-world networks – ranging from social and biological to technological systems – that modular, local, structures can drive global activities and function, e.g. disease spread over contact networks [5, 15, 16], coordination in starling flocks [6], power distribution across Europe [17], and time consensus over satellite constellations [4].

We introduce a local eigenvector centrality that considers the most topologically relevant scale for detecting node centrality, in reference to prominent eigengaps, such that the set of eigenvectors used to produce the new centrality reflects a local, community-considerate, assessment. The role of eigenvalues and their eigengaps in identifying prominent community structures can be understood through the following analogy to a physical system. Consider a spring system with two densely connected hubs and only a few connections between these two communities. By pulling such a

structure apart in two separate directions, according to the second eigenvector, the hubs can be kept physically separate from each other at a relatively large distance. The second eigenvalue reflects this physical separation and so has a relatively large value. To pull the same structure in three distinct directions would be more difficult, with no clear division into three groups resulting in at least one of the densely connected communities being split into two sets of nodes. Therefore, the third eigenvalue would be relatively small as at least two of the three defined communities are still in close proximity. This produces a large difference between the magnitude of the second and third eigenvalues. Monitoring these differences, referred to as eigengaps or spectral gaps, provides insight into the community structure of any given graph.

Eigengaps are employed in community detection algorithms, including spectral clustering, where the eigengap is used as a heuristic to guide cluster detection [10]. Spectral clustering embeds a network in a Euclidean space defined by the graph’s eigenvectors, with algorithms such as k-means being applied to detect node clusters. Spectral embeddings and eigengap analysis have been employed across a range of studies where the choice of network matrix representation has been shown to be influential. In [18], the normalised Laplacian was identified as the most effective for determining community presence from its eigengaps, following comparisons with adjacency, Laplacian, modularity and correlation matrices. Similarly in [8] the most effective machine learned embeddings for community detection were found to closely resemble the spectral embeddings generated from the normalised Laplacian matrix. In detecting communities of dynamical influence [6], the direct relationship between the Laplacian matrix and the detection of effective leadership was demonstrated. The adjacency matrix has also been applied to perform clustering in reference to the largest eigengap, where node correlations from an extended set of eigenvectors determined partitions [9]. Herein, the adjacency matrix is used to identify centrality in terms of reach and connectivity which is distinct from the notion of leadership and dynamical influence [6, 14].

Eigenvector centrality was notably adapted for use in Google’s PageRank algorithm [12]. PageRank can be conceptualised as an assessment of random walkers traversing a graph to determine the popularity of nodes as a destination, where at each node the probability of traversing an outgoing edge is based on relative edge weightings. Eigenvector centrality has a similar conceptualisation, but instead of probabilistic flow it is the absolute edge weightings that govern the flow and assessment of node centrality. Issues arise with eigenvector centrality, referred to as localisation effects, where the centrality of densely connected hubs and isolated communities are amplified, i.e. similar to random walkers becoming trapped in an area of the graph and repeatedly visiting the same set of nodes [13]. PageRank – with its random teleportation function – and the non-backtracking (Hashimoto) matrix [1, 13] – that prevents return along traversed edges – have been developed in part to mitigate localisation in the calculation of centrality. Local eigenvector centrality is not developed to avoid the issue of localisation but mitigation strategies are presented herein.

The local eigenvector centrality provides a refined measure of node importance that adapts to the underlying community structure within a graph. It extends Bonacich’s eigenvector centrality [2] and conceptually relates to eigengap-aware spectral clustering methods [10, 18]. While spectral clustering – such as k-means-based approaches – partitions a graph into distinct communities, local eigenvector centrality reflects the interplay of centrality within and across communities without explicitly defining them.

2 Methodology

An adjacency matrix, A , is a square $n \times n$ matrix representing a graph of n vertices, where $a_{ij} > 0$ (with a_{ij} the (i, j) -th entry of the graph's adjacency matrix) if there exists a directed edge from vertex i to j , and 0 otherwise.

The local eigenvector centrality is defined in reference to a prominent eigengap – often the largest real eigengap that responds to the most prominent community structures in the graph [18] – among the eigenvalues $\lambda_1, \lambda_2, \dots, \lambda_n \in \mathbb{C}$ of A , where we assume the ordering

$$\operatorname{Re}(\lambda_1) \geq \operatorname{Re}(\lambda_2) \geq \dots \geq \operatorname{Re}(\lambda_n). \quad (1)$$

The real component of each eigenvalue provides information on the size of the transformation of A in a given direction, defined by the associated eigenvector. We define the i -th eigengap as

$$g_i = \operatorname{Re}(\lambda_i) - \operatorname{Re}(\lambda_{i+1}). \quad (2)$$

When the presence or prominence of communities in a graph is unknown, we are interested in identifying the largest eigengap. Specifically, we are interested in the relative scaling applied by adjacent eigenvalues to their eigenvectors. Hence, we constrain our eigengap search to nonnegative eigenvalues that do not also reverse the direction of the eigenvectors, denoted as

$$k = \arg \max_{\operatorname{Re}(\lambda_i) > 0} g_i. \quad (3)$$

If two eigengaps are the same, as may happen for bipartite graphs for example, we select k as the smallest index realising the maximum eigengap. The smaller index corresponds to larger structures in the graph.

To define our local eigenvector centrality measure, we introduce a variant of the matrix of eigenvectors. Recall that each distinct eigenvalue λ of A is associated with at least one eigenvector $x \neq 0$, satisfying $Ax = \lambda x$. Since A is real, complex eigenvalues appear in conjugate pairs, and so do the corresponding eigenvectors, i.e.,

$$Ax = \lambda x \iff Ax^* = \lambda^* x^*. \quad (4)$$

Moreover, because of the above ordering, conjugate pairs of eigenvalues correspond to consecutive indices in our list.

We build a matrix

$$V = [v_1 \mid v_2 \mid \dots \mid v_k] \in \mathbb{R}^{n \times k} \quad (5)$$

according to the following rules:

- If $\lambda_i \in \mathbb{R} \setminus \{0\}$, then $v_i \in \mathbb{R}^n$ satisfies $Av_i = \lambda_i v_i$ and $\|v_i\|_2 = 1$.
- If $\lambda_i \in \mathbb{C}$, then $\lambda_{i+1} = \lambda_i^*$ and

$$v_i = \frac{\operatorname{Re}(x)}{\|\operatorname{Re}(x)\|_2}, \quad v_{i+1} = \frac{\operatorname{Im}(x)}{\|\operatorname{Im}(x)\|_2}, \quad (6)$$

where $x \in \mathbb{C}^n$ is the eigenvector associated with λ_i with $\|x\|_2 = 1$.

- If $\lambda_i = 0$, then $v_i = 0$.

This matrix V uses information from the eigenvectors of A but is not itself a matrix of eigenvectors; indeed, neither the zero vector nor the real/imaginary parts of a complex eigenvector are eigenvectors of A .

With this notation, the vector of local eigenvector centralities c is defined as

$$c(i) = \sqrt{\sum_{j=1}^k v_j(i)^2} = \|[v_1(i), \dots, v_k(i)]\|_2 = \|e_i^\top V\|_2, \quad (7)$$

where e_i is the i -th standard basis vector of \mathbb{R}^n , with $e_i(i) = 1$ and 0 elsewhere.

Remark: The above construction implicitly assumes that all the eigenvalues of A up to the k -th are semi-simple, i.e., that their algebraic and geometric multiplicities coincide. This is not always the case, as eigenvalues may be repeated s times in the spectrum but have $< s$ associated linearly independent eigenvectors. In such scenarios (when an eigenvalue is defective), we only consider the eigenvectors returned.

The local eigenvector centrality is developed for application to the adjacency matrix, as is the nominal usage of eigenvector centrality. However, the Laplacian matrix L is another common graph representation, defined as

$$L = D - A, \quad (8)$$

where D is the degree matrix. Variants such as the normalised Laplacian, L_{norm} , are proposed as effective models for community detection [18], particularly in graphs with heterogeneous degree distributions [8]. The normalised Laplacian is defined as

$$L_{\text{norm}} = I - D^{-1/2} A D^{-1/2}. \quad (9)$$

2.1 Complex Conjugates

Complex conjugate pairs are rationalised in the context of centrality and community structure by considering the role of eigenvectors in decomposing a graph into a number of components corresponding to a given eigenvector, i.e. third eigenvector v_3 would identify decomposition into three separate node groupings. When there exist multiple valid configurations for allocating nodes into ℓ components in the graph, and/or no clear configuration into ℓ components, then complex conjugates arise. Such a case is displayed in Figure 1, where four communities are clearly visible in this toy example both in the eigengap analysis (Figure 1a) and the local eigenvector centrality result (Figure 1b). The first and fourth eigenvectors (Figure 1c and f) have real eigenvalues with Figure 1f depicting the decomposition of the graph into four communities. There is no way to decompose the graph into three balanced communities. As a result, the second and third eigenvectors have corresponding entities that are complex conjugate pairs, whereby the Real components of both eigenvectors identify one configuration of dividing the graph into two components and the Imaginary value components identify the other configuration.

This informs the local eigenvector centrality methodology, whereby complex conjugate pairs should be identified and replaced with two vectors based on the normalized Real and Imaginary component of one of the eigenvectors. Note that only the relative sign of the eigenvector entries is important, so either of the complex conjugate eigenvectors can be used to generate the two replacement vectors.

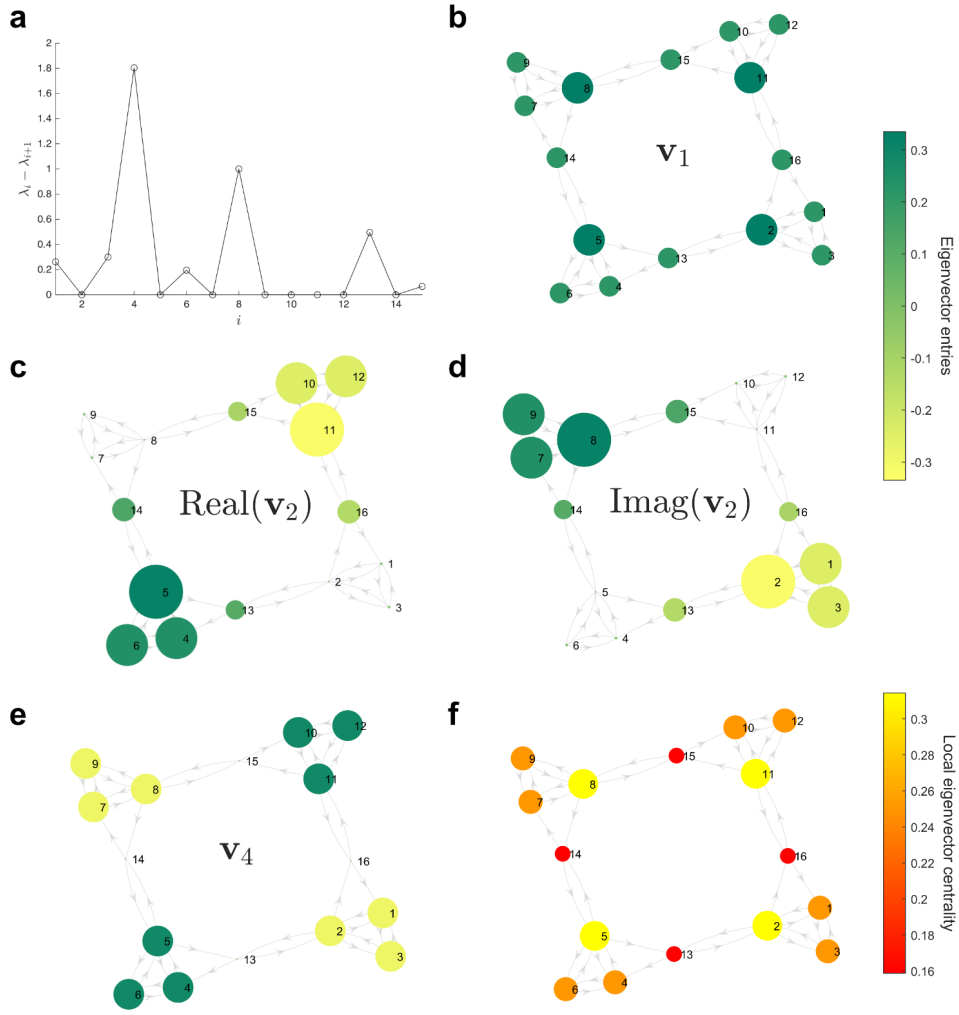


Figure 1: A four community graph example, where the complex conjugate pair occur at v_2 and v_3 , with the real and imaginary values of v_2 displayed. (a) Eigengap analysis, (b) first eigenvector v_1 , (c) absolute real component of v_2 , (d) absolute imaginary component of v_2 , (e) absolute v_4 values, and (f) local eigenvector centrality.

2.2 Directed Path

A directed path presents another edge case, where this directed acyclic graph takes the following form:

$$A = \begin{bmatrix} 0 & 1 & 0 & \cdots & 0 \\ 0 & 0 & 1 & \cdots & 0 \\ \vdots & \vdots & \vdots & \ddots & \vdots \\ 0 & 0 & 0 & \cdots & 1 \\ 0 & 0 & 0 & \cdots & 0 \end{bmatrix}. \quad (10)$$

In this configuration, there is a single eigenvalue of A that is equal to zero. Since an eigenvalue of zero indicates that the associated eigenvector corresponds to a direction of null transformation under the adjacency operator, this eigenvector offers no useful information for centrality analysis. Therefore, there is no centrality analysis possible in this example, and in the more general case, eigenvectors corresponding to zero eigenvalues should be excluded by setting their entries to zero.

2.3 Directed Cycle

A directed cycle provides an edge case for evaluating the proposed local eigenvector centrality and takes the following form:

$$A = \begin{bmatrix} 0 & 1 & 0 & \cdots & 0 \\ 0 & 0 & 1 & \cdots & 0 \\ \vdots & \vdots & \vdots & \ddots & \vdots \\ 0 & 0 & 0 & \cdots & 1 \\ 1 & 0 & 0 & \cdots & 0 \end{bmatrix}, \quad (11)$$

where the eigenvectors are complex conjugate pairs, except for the largest eigenvalue in a graph of odd order and for both the largest and smallest eigenvalues in a graph of even order.

The cyclic nature of the graph also results in the largest eigengap being located centrally in the eigengap order, as depicted in Figure 2 for a 10-node directed cycle. However, the combination of eigenvectors (eigenvectors 1 to 5 for a 10-node directed cycle) produces a local eigenvector centrality of equal values, which is also equal to the eigenvector centrality (i.e., v_1).

Both centrality measures correspond to the intuition that all nodes have equal influence in this cyclical graph.

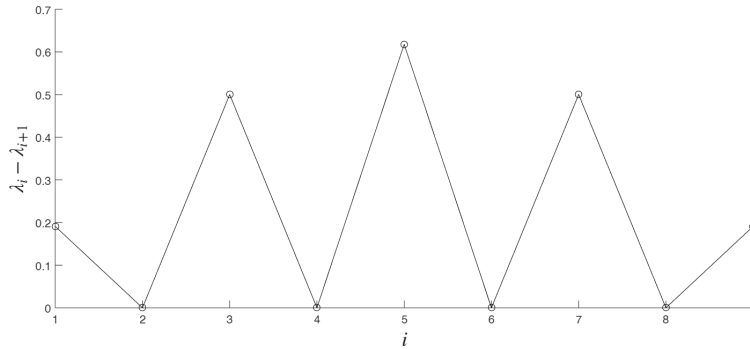


Figure 2: Eigengaps for a 10-node directed cycle

2.4 Road networks

This study includes the analysis of road networks that are constructed from open-source geospatial data using OpenStreetMap (OSM). A motor-vehicle-accessible graph was extracted from OSM via the OSMnx `graph_from_place` function by restricting to the drive network type. The resulting graph is composed of road intersections as nodes and road links as edges. Edges have length and speed limit attributes that can be used to compute approximate travel times. If these travel times exceed what is possible, for an average car accelerating at 2 m/s^2 from stationary, then the travel time, t , is estimated according to $t = \sqrt{\frac{2d}{a}}$ where d is the distance and $a = 2 \text{ m/s}^2$.

The OSM-derived graph is then converted into an undirected adjacency matrix, A , given the largely bidirectional nature of road networks and to avoid cul-de-sacs skewing centrality results. The weighting of the adjacency are based on the inverse of the travel times between nodes, t_{ij} for nodes i and j , such that large weights correspond to shorter travel times. To mitigate distortions caused by short links, such as at roundabouts and motorway on/off ramps, the weights are defined as,

$$a_{ij} = \frac{1}{1 + t_{ij}}. \quad (12)$$

If the relationship was simply $1/t_{ij}$, then the function would become unbounded as $t_{ij} \rightarrow 0$.

3 Results

Local eigenvector centrality is proposed to more accurately capture the distribution of node centrality in networks with prominent community structure. This local centrality measure is first evaluated in networks with known, well-defined, community structure before being demonstrated on networks where communities can be anticipated but are not clearly defined.

3.1 Defined community structure

In a school, community structure is shaped by the year and class structure, where students spend more time with peers and classmates. Primary school, [19] and High School [11] contact networks provide excellent testbeds for showing how local eigenvector centrality responds to defined community structures.

For the Primary School, Figure 3a displays how prominent eigengaps align with the breakdown of the contact network into 5 year-groups and 10 classes. The eigengap analysis also suggests that despite the year and class structure, pupils across the school are closely connected given that the largest eigengap is at $i = 1$. Class 1B is shown to be the most globally central and well-connected class in Figure 3b. The local eigenvector centrality is identified for both the $i = 5$ and 10, corresponding with prominent eigengaps in Figure 3a. For local ($i = 5$) in Figure 3c, each year group contains relatively high centrality nodes including years 3–5 that report negligible eigenvector centrality. The expansion to $i = 10$ in Figure 3d delivers similarly high centrality nodes in all 10 classes.

We can compare local eigenvector centrality with the results of eigenvector centrality identified for each class independently, since we know which pupils belong to each class. In Figure 4a, we present this comparison for the ten subnetworks associated with the ten classes – referred to as Class eigenvector centrality – and overlay these results on those of local eigenvector centrality applied at $i = 10$. The differences in centrality distribution with respect to both class eigenvector centrality and PageRank are visualised in Figure 4b and c. These comparisons highlight where

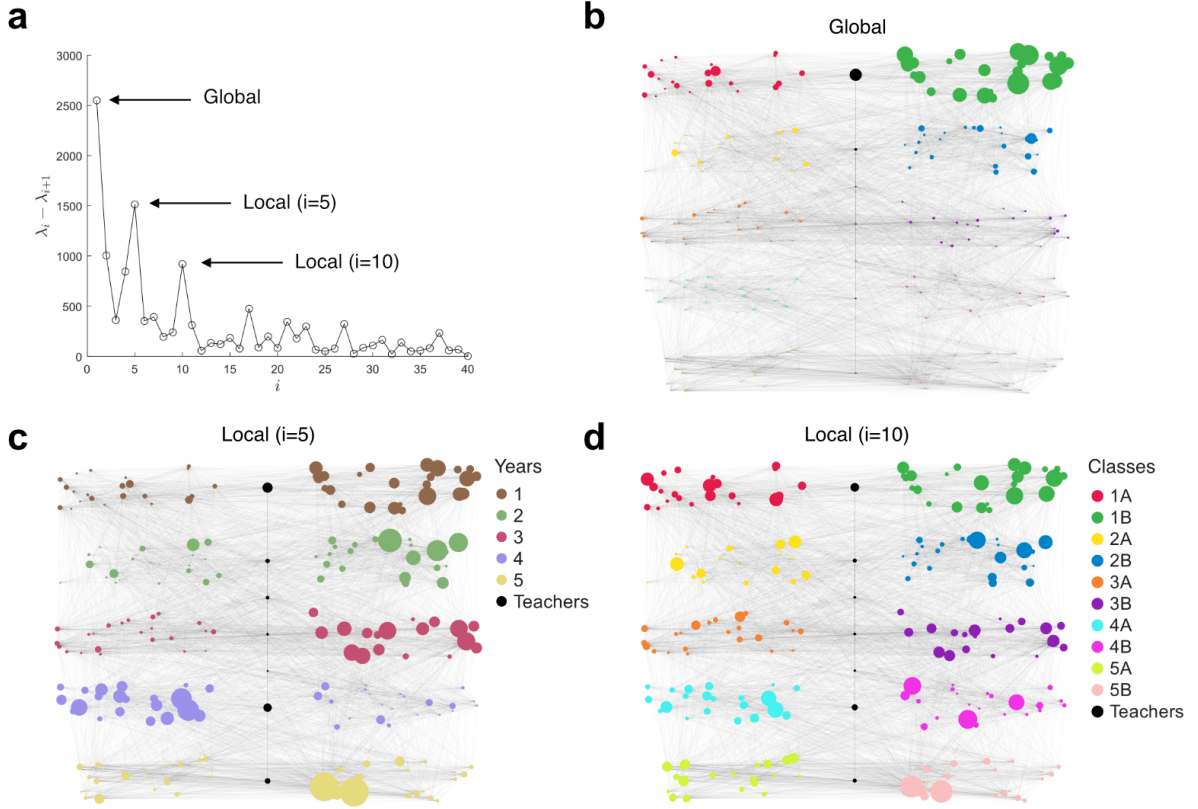


Figure 3: Centrality analysis of the Primary School contact network. (a) Eigengap plot showing prominent eigengaps at $i = 1, 5$, and 10 . (b) Eigenvector centrality distribution capturing global centrality. (c) Local eigenvector centrality for $i = 5$. (d) Local eigenvector centrality for $i = 10$. In panels (b–d), the circle sizes are proportional to the corresponding centrality values, highlighting the relative importance of each node within the network.

discrepancies exist, with the centrality distributions presenting as largely similar with PageRank diverging consistently only at high local eigenvector centrality values. Following median absolute deviation (MAD) normalisation, we compute the Euclidean distance, d , between local eigenvector centrality, x , and class eigenvector centrality, y , and between x and PageRank, z . These result shows a closer match for class eigenvector centrality, $d(x, y) = 13.0$, than PageRank, $d(x, z) = 18.3$. This finding is further supported by visualising the centrality difference boxplots in Figure 4c, which show that the majority of class eigenvector values fall within one MAD. Local eigenvector centrality emulating the centrality distribution of each class’ eigenvector centrality, without *a priori* knowledge of the class structure.

Discrepancies between the class and local centrality measures are to be expected. Local eigenvector centrality reflects local community structure but it also accounts for connections across classes and with teaching staff. Class eigenvector centrality in contrast only considers connections within each class. The most globally connected class, according to Figure 3b, is class 1B. Therefore, the local eigenvector centrality values are higher than class eigenvector centrality for a number of the nodes with strong connections across the school. These nodes are also visible in Figure 4b as rising blue spikes between indices 50–100. Inversely, class 2A does not appear prominently in

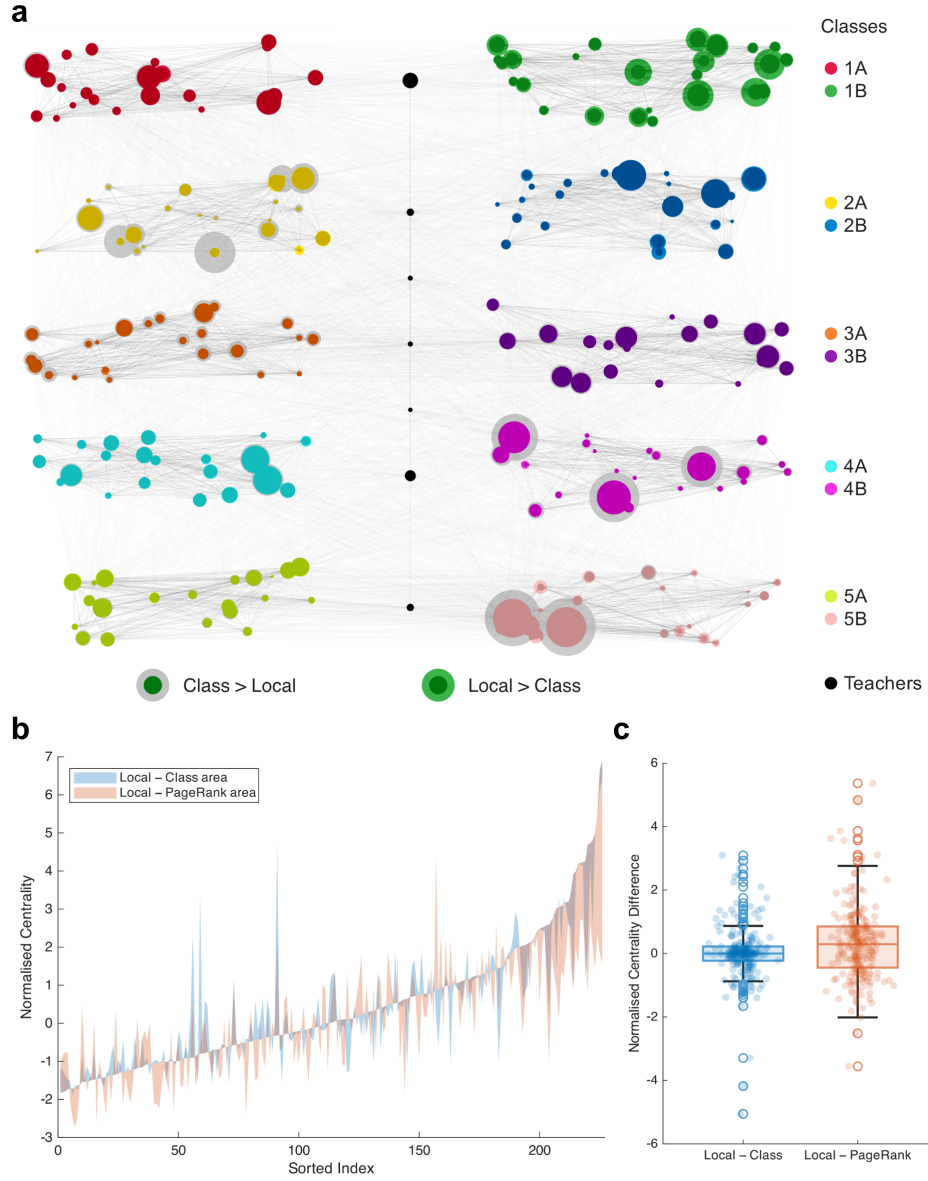


Figure 4: Comparison of each class eigenvector centrality with local eigenvector centrality, $i=10$, for the Primary School network where circle sizes are proportional to the corresponding centrality values, (b) class eigenvector centrality and PageRank difference with respect to sorted local eigenvector centrality values, and (c) boxplot of the class eigenvector centrality and PageRank differences.

class or local eigenvector centrality measures in Figure 3. Class eigenvector centrality is a relative measure, so analysis of the class 2A in isolation detects nodes that are central within that class even if they are not well connected beyond it.

PageRank is also expected to differ from eigenvector-based centrality, given its emphasis on probabilistic flow versus absolute flow assessment from eigenvector centrality. PageRank's teleportation function, set to 0.85 here, provides a more even spread of centrality, i.e. mitigating the

localisation of centrality values. The latter contributes to the main source of discrepancy between PageRank and Local eigenvector centrality in Figure 4b, where PageRank consistently attributes lower centrality scores to the highest local eigenvector centrality nodes.

In Figure 5, the eigengaps of a High School contact network, [11], do not align with the three defined classes (PC, PC*, and PSI*), but local connectivity is prominent with the largest gap at $i = 5$. This unexpected eigengap can be explained by comparing the local eigenvector centrality with

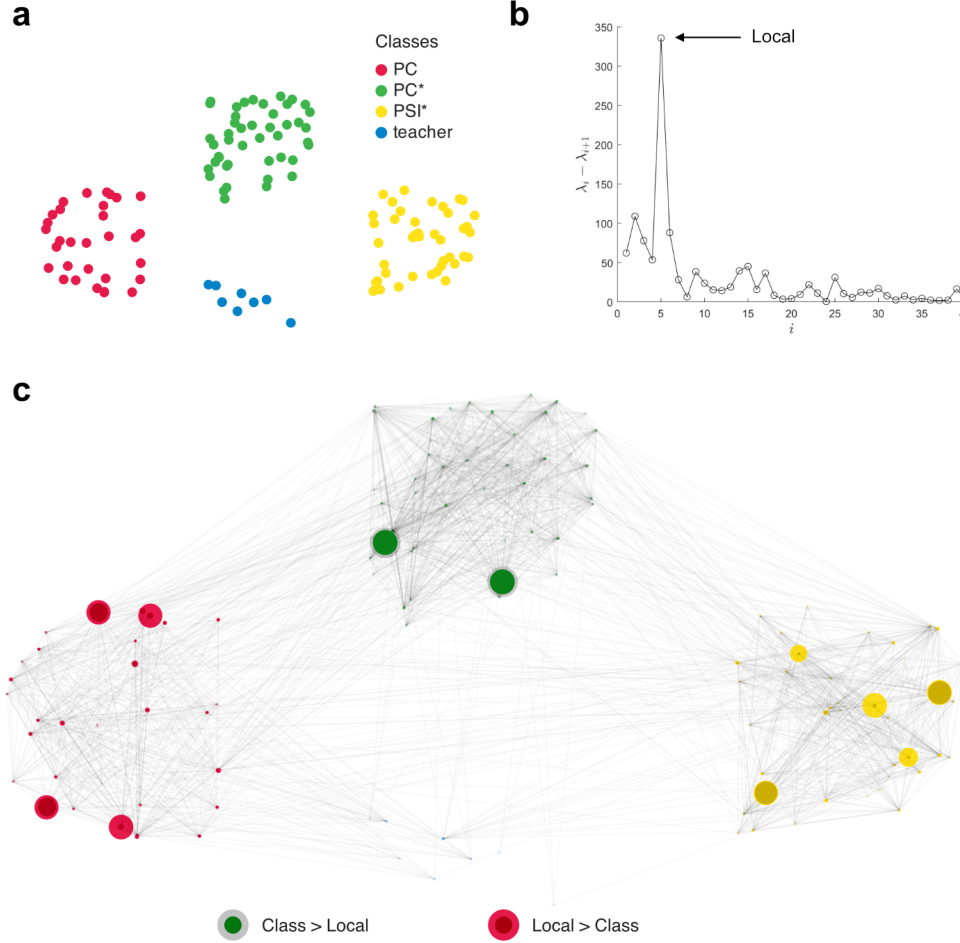


Figure 5: Centrality analysis of a High School contact network. (a) Visualisation of class membership. (b) Eigengap plot showing prominent eigengap at $i = 5$. (c) Comparison of each class eigenvector centrality with local eigenvector centrality for $i = 5$. Circle sizes are proportional to the corresponding centrality values, illustrating the relative centrality of nodes according to these measures.

class eigenvector centralities. Differences between these assessments provide additional insights on the source of a node's centrality. Nodes that are central within their known community, but weakly connected beyond it, have higher class eigenvector centrality. While, nodes that are primarily connected to nodes outside of their known community have higher local eigenvector centrality and indicate the presence of hidden community structures. The prominent nodes where $\text{Local} > \text{Class}$ in the PC and PSI* classes are central due to prominent connections outside of their class. As

a result, the nodes are identified in two separate eigenvectors that are responsible for the largest eigengap at $i = 5$ despite the three class structure.

3.2 Localisation mitigation

For the High School network, PageRank provides a notably different assessment of centrality than Local and class eigenvector centrality. PageRank avoids localisation and therefore distributes centrality more evenly across the network, visualised in Figure 6a as a grey overlay, than was seen in Figure 5c. However, by performing a non-linear rescaling of local eigenvector centrality, x , as

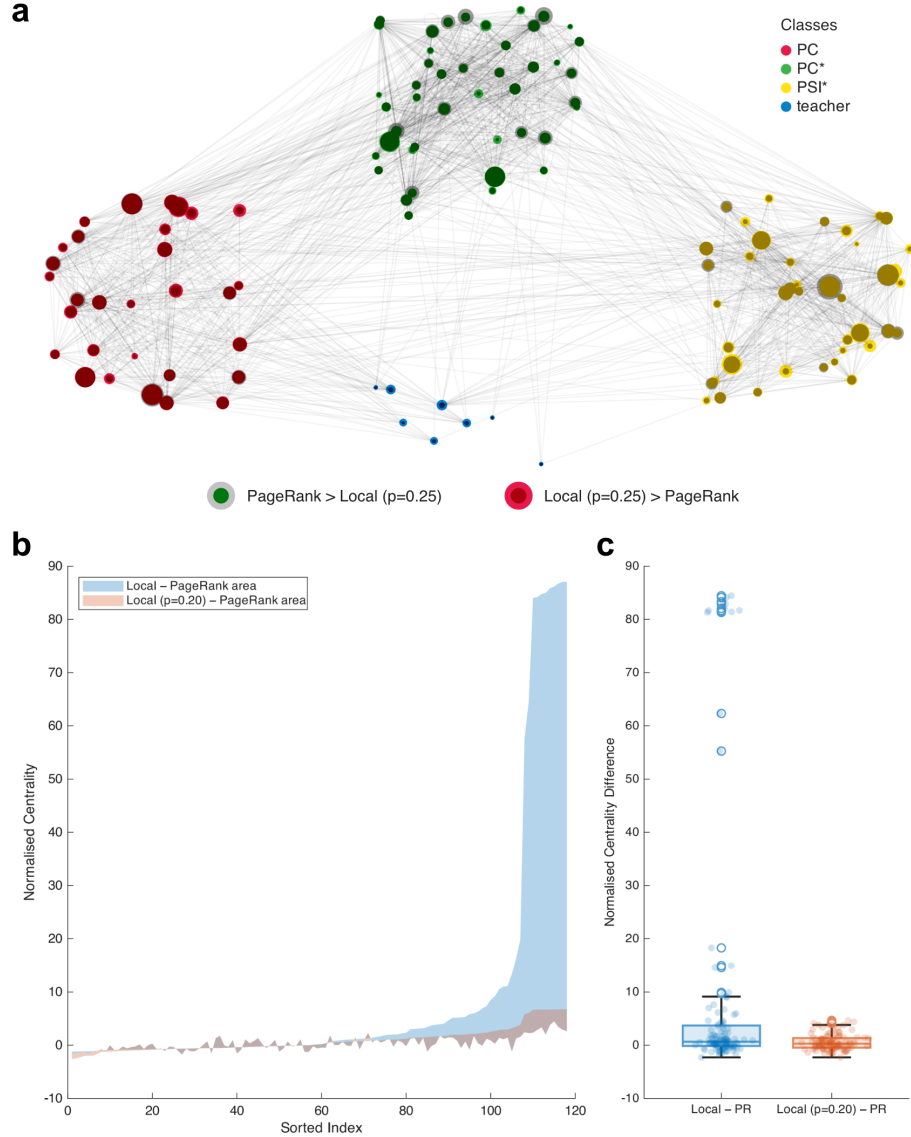


Figure 6: Comparison of (a) PageRank with local eigenvector centrality ($i=5$) for the High School network where circle sizes are proportional to the corresponding centrality values. Local eigenvector centrality, without and with $p=0.2$ non-linear rescaling, comparison with PageRank (PR) displayed as (b) difference area plot and (c) boxplot.

$$\mathcal{N}_p(x) = \frac{x^{\circ p}}{\sum x^{\circ p}} \quad (13)$$

where $x^{\circ p}$ is an element-wise Hadamard power, a similar distribution can be obtained for the local eigenvector centrality ($p = 0.2$). The minimum power was determined by minimising the Euclidean distance, d , with respect to PageRank, z . For $p = 0.2$, the distance $d(\mathcal{N}_{0.2}, z) = 17.1$ is similar to the Primary School comparison and much smaller than with the initial centrality $d(\mathcal{N}_1, z) = 264.4$. The main area of discrepancy after non-linear rescaling remains the high centrality values, as in Figure 4b. There is a clear rationale for discrepancies between class and local eigenvector centrality. The variation between PageRank and local eigenvector centrality is affected by differences in assessment between probabilistic and absolute flow, as well as the teleportation function. The latter promoting a more even distribution of centrality, but the largest differences are still found in high centrality values when teleportation is not enabled when applying PageRank.

3.3 Undefined community structure

Local eigenvector centrality is applied to the adjacency matrix representing a road network, as described in Section 2.4, to demonstrate the insights that can be obtained when community structure is unknown or not clearly defined.

High centrality values are denoted for the city of Glasgow, UK, in Figure 7 where the largest eigengap $k = 7$ indicates the lack of global connectivity. Localisation effects due the scale of the graph, $n = 12,979$, are mitigated in Figure 7 by applying non-linear scaling to local eigenvector centrality, $p = 0.2$. This expands the visible centrality distribution to more clearly identify the contributing junctions and region associated with each highly central location. The local eigenvector centrality assessment highlights seven junctions of high centrality that correspond to three junctions around the city centre (the top left city centre location is identified by Bonacich's eigenvector centrality), one prominent junctions in the city's west end (Maryhill), two in the southside of the city (Darnley, Battlefield) and one in the South-West (Govan) that connects the motorway to the Clyde Tunnel. The asymmetrical motorway layout, with greater access in the East end, likely influences the prominence of high centrality junctions on the less accessible west and south side of the city.

The nodes identified by eigenvector centrality are adjacent to the city centre and in closest proximity to the motorway from those highlighted city centre junctions in Figure 7. Note that weighting network edges according to an inverse travel time relationship often results in motorway sections with lower weightings than close proximity junctions.

Glasgow prominent community structure is likely due to a range of factors, including Glasgow's growth integrating multiple villages and towns, a halted motorway redevelopment, and a lack of coordination between national and regional governance [7].

3.4 Differing insights from the Laplacian

In [18], the normalised Laplacian was identified as the most effective for determining community presence from its eigengaps. Similarly [8] found that the most effective machine learned embeddings for community detection closely resembled the spectral embeddings generated from the normalised Laplacian matrix. Hence, a case could be made for using the normalised Laplacian as the basis for a local eigenvector centrality. However, as discussed with respect to directed paths, Section 2.2, the Laplacian represents consensus dynamics and its eigenvectors highlight the nodes that can most effectively drive that collective response. Therefore, adapting the local eigenvector centrality assessment to employ the normalised Laplacian does not identify central locations and prominent

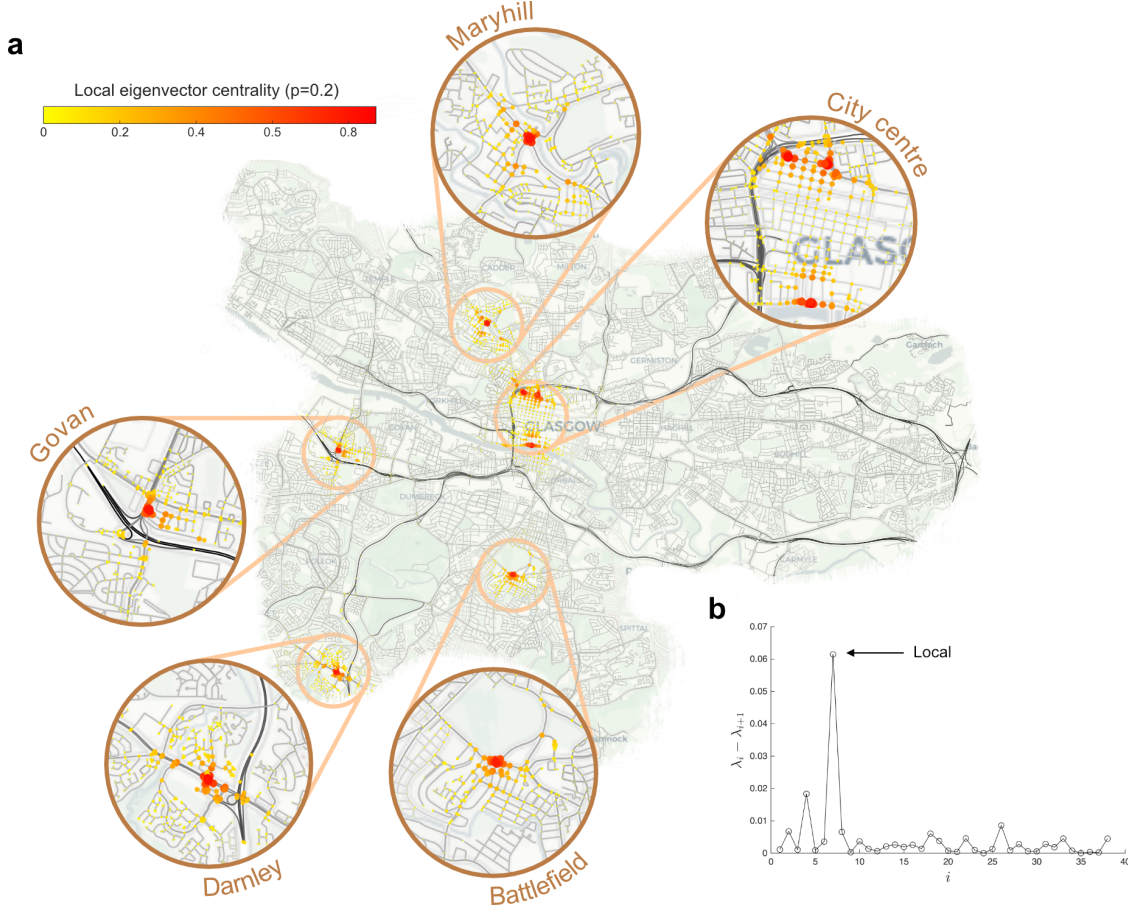


Figure 7: Local eigenvector centrality for the Glasgow road network. (a) Map of Glasgow with road speed limit denoted in grayscale (20–70 mph). Local eigenvector centrality values are displayed, which includes the nodes highlighted by eigenvector centrality. (b) Eigengap analysis showing the largest eigengap $k = 7$.

junctions as is the case when using the adjacency in Figure 7. Instead, for the Glasgow road network, the Laplacian-based local eigenvector centrality shown in Figure 8 attributes the highest centrality to the most isolated communities in the graph. These communities are located around the edge of the network, and often only accessible through a single road bottleneck. With the Laplacian representing consensus dynamics, this high centrality is an acknowledgment that isolated communities require local leadership due to their lack of global connectivity [6]. This does not translate to the notion of centrality as detecting highly connected regions of the graph that receive significant traffic flow.

4 Discussion

Centrality is always considered within a bounded sphere of influence, usually clearly defined by the extent of the network. In complex networks, the topology is often not well characterised or understood; hence, the scale at which centrality is most relevant is less clear. For example, a study of the primary school’s contact network noted high connectivity within the year groups that coincided with an expected increase in local connections within the classes [19]. Without knowledge

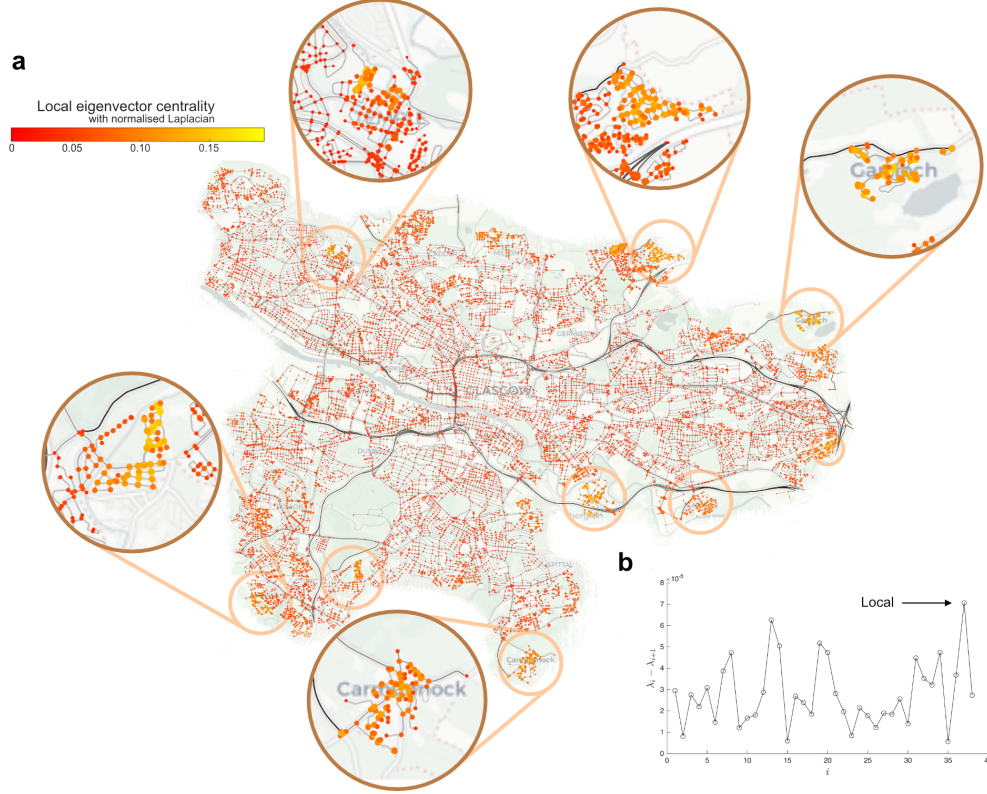


Figure 8: Local eigenvector centrality based on the normalised Laplacian of the Glasgow road network. (a) Map of Glasgow with road speed limit denoted in grayscale (20–70 mph) and Local eigenvector centrality values displayed. (b) Eigengap analysis showing the largest eigengap $k = 37$.

of the class structure, eigenvector centrality points towards the dominant presence of class 1B in Figure 3b with no central actors within years 4 and 5. In reality, each class and year group is likely to have central nodes within those communities. The local eigenvector centrality manages to capture centrality at both a year and class scale for this example, Figure 3c and d respectively. The centrality distributions at class-level validated through comparison with eigenvector centrality applied for each class subnetwork in isolation, see Figure 4.

An eigengap assessment is a key step in determining a local eigenvector centrality. As noted by [18, 10], the presence of the largest eigengap at an index greater than 1 indicates prominent community structure. The Primary School example in Figure 3 demonstrates how a more nuanced picture of community structure emerges by investigating multiple prominent eigengaps that respond to known community structures. The largest eigengap is located at $k = 1$, but prominent eigengaps are also found at $i = 5$ and $i = 10$ that reveal centrality distributions that respond to year groups and classes. Similarly, for road networks or other examples where an edge weighting must be defined in order to evaluate centrality, the eigengap distribution can vary depending on that edge weighting selection. Therefore, the largest eigengap does not provide a definitive answer on the presence of community structure. The edge weightings defined in Eq. 12 capture an inverse relationship to travel time that aligns with the notion of centrality. This relationship prevents the function from becoming unbounded when travel times between nodes are very small and produces a largest eigengap at $k = 7$ for the Glasgow road network in Figure 7. By selecting a simpler inverse relationship $1/t_{ij}$ that allows for relatively large weightings on short connections,

the largest eigengap appears at $k = 1$ with the next most prominent eigengap clearly defined at $i = 7$. Despite the differing locations of the largest eigengap, both eigengap distributions are suggestive of community structure in the Glasgow road network when the full eigengap distribution is considered.

The Laplacian matrix, and particularly the normalised Laplacian, is often promoted as the most reliable representation for eigengap-based community detection and clustering [18, 10]. However, a Laplacian-based centrality is influenced to a greater extent by isolated regions in a graph, which makes it less suitable as a centrality measure. The Laplacian matrix captures consensus dynamics with the consequence that Laplacian eigenvectors identify nodes required to drive a collective response [6, 14]. The nodes and communities with high Laplacian eigenvector entries are either highlighted due to their centrality or their isolation. The latter does not conform to the notion of centrality as a measure of highly-connected nodes that are central to prominent cycles within the network, i.e. high volume of traffic/flow. The adjacency matrix presents a better alignment to this notion of centrality by modelling the propagation of influence across the network. The adjacency is therefore better suited to calculation of local eigenvector centrality.

The adjacency eigenvectors, selected according to prominent eigengaps, are found to reflect known structures in the graph for the school contact networks. Clustering using the adjacency matrix was found to be most effective when employing a larger set of eigenvectors than would be suggested by the largest eigengap [9]. This suggests that not all communities will be prominently represented by a local eigenvector centrality assessment. For example, less well-connected communities may have no nodes with high centrality. In this way, local eigenvector centrality is not a community detection or clustering algorithm, but an assessment of centrality that integrates local and global connectivity.

The localisation of adjacency eigenvectors diminish the usefulness of eigenvector-based centrality measures. Non-backtracking matrices [1, 13] and PageRank [12] were developed to mitigate localisation effects. PageRank has been used here as a reference measure for correcting localisation in local eigenvector centrality through non-linear rescaling. Although the basis of eigenvector and PageRank centrality measures are only subtly different, there is additional value from local eigenvector centrality’s deterministic integration of local and global influence. Comparisons with eigenvector centrality applied at a subnetwork/community level provides insights into the source of node centrality. The deconstruction of this local centrality into its contributing eigenvectors further distinguishes itself from PageRank that lacks an explicit link to community structure. Instead community structure is accounted for, but not characterised, through the teleportation function.

5 Conclusion

Local eigenvector centrality is a vital expansion on the established eigenvector centrality, reflecting not just global connectivity but also the interplay with locally prominent community structures. When communities are known or clearly defined, local eigenvector centrality produces a similar centrality assessment to the eigenvector centrality calculated for each known community in isolation. Local eigenvector centrality also captures the node and community hierarchy in terms of global reach and centrality. Therefore, comparing the local and community subnetwork centralities provides insights into the relative connectivity of a node within its defined community versus its prominence in the wider network.

Localisation effects constrain the usefulness of eigenvector centrality. PageRank performs a distinct but similar assessment of centrality to eigenvector-based measures. The similarity enables PageRank to act as an effective reference for correcting localisation in local eigenvector central-

ity, via non-linear rescaling, as the centrality distributions are highly similar in networks where localisation is minimal.

Local eigenvector centrality identifies nodes that experience high volumes of traffic and flow both locally and globally, by analysing the eigenspectrum of the adjacency matrix. These are distinct insights from the eigenspectrum of the Laplacian matrix, where communities can be prominent due to their isolation and need for local consensus leadership.

6 Data availability

Code and example datasets used in this study are currently available in a GitHub repository: https://github.com/RuaridhClark/Local_eigenvector_centrality. The repository contains MATLAB and Colab notebooks, as well as the datasets analysed in the paper. The code and data will be archived on Zenodo following paper acceptance to obtain a permanent DOI.

References

- [1] F. Arrigo, D. J. Higham, and V. Noferini. Beyond non-backtracking: non-cycling network centrality measures. *Proceedings of the Royal Society A*, 476:20190653, 2020.
- [2] P. Bonacich. Factoring and weighting approaches to status scores and clique identification. *Journal of mathematical sociology*, 2:113–120, 1972.
- [3] P. Bonacich. Some unique properties of eigenvector centrality. *Social Networks*, 29:555–564, 2007.
- [4] A. Bouis, R. A. Clark, and M. Macdonald. Insights on structure and influence from the adjacency and laplacian eigenspectra of intersecting ring networks. *arXiv preprint arXiv:2505.21294*, 2025.
- [5] R. A. Clark and M. Macdonald. Identification of effective spreaders in contact networks using dynamical influence. *Applied Network Science*, 6:5, 2021.
- [6] R. A. Clark, G. Punzo, and M. Macdonald. Network communities of dynamical influence. *Sci Rep*, 9:17590, 2019.
- [7] B. Cox. *Designing the streets of the future: The Avenues Programme, Glasgow*. PhD thesis, University of Glasgow, 2024.
- [8] S. Kojaku, F. Radicchi, Y.-Y. Ahn, and S. Fortunato. Network community detection via neural embeddings. *Nature Communications*, 15:9446, 2024.
- [9] M. Lucińska and S. T. Wierzchoń. Clustering based on eigenvectors of the adjacency matrix. *International Journal of Applied Mathematics and Computer Science*, 28, 2018.
- [10] U. V. Luxburg. A tutorial on spectral clustering. *Statistics and computing*, 17:395–416, 2007.
- [11] R. Mastrandrea, J. Fournet, and A. Barrat. Contact patterns in a high school: A comparison between data collected using wearable sensors, contact diaries and friendship surveys. *PLOS ONE*, 10:1–26, 10 2015.

- [12] L. Page, S. Brin, R. Motwani, and T. Winograd. The pagerank citation ranking: Bringing order to the web. Technical report, Stanford infolab, 1999.
- [13] R. Pastor-Satorras and C. Castellano. Distinct types of eigenvector localization in networks. *Scientific Reports*, 6, 2016.
- [14] G. Punzo, G. F. Young, M. Macdonald, and N. E. Leonard. Using network dynamical influence to drive consensus. *Scientific reports*, 6:26318, 2016.
- [15] P. Sah, S. T. Leu, P. C. Cross, P. J. Hudson, and S. Bansal. Unraveling the disease consequences and mechanisms of modular structure in animal social networks. *Proceedings of the National Academy of Sciences of the United States of America*, 114, 2017.
- [16] M. Salathé and J. H. Jones. Dynamics and control of diseases in networks with community structure. *PLOS Computational Biology*, 6:1–11, 10 2010.
- [17] M. T. Schaub, J.-C. D. S. N. Yaliraki, and M. Barahona. Markov dynamics as a zooming lens for multiscale community detection: Non clique-like communities and the field-of-view limit. *PLOS ONE*, 7:1–11, 10 2012.
- [18] H.-W. Shen and X.-Q. Cheng. Spectral methods for the detection of network community structure: a comparative analysis. *Journal of Statistical Mechanics: Theory and Experiment*, 2010:P10020, 2010.
- [19] J. Stehlé, N. Voirin, A. Barrat, C. Cattuto, L. Isella, J.-F. Pinton, W. Q. Marco, V. den Broeck, C. Régis, P. L. Bruno, and Vanhems. High-resolution measurements of face-to-face contact patterns in a primary school. *PLOS ONE*, 6:e23176, 10 2011.